integration schemes may be checked. It is important that the solution for φ depends on one (prescribed) parameter λ only. Once solved, an infinite number of solutions can be generated directly by adjusting A_0. In this sense, Φ is defined by a two-parameter family of solutions. Because $dA/dt=\lambda\neq 0$, the solution would correspond to an initially "steady" solution with an "impulse" at $t=0+$. For $\lambda=0$, of course, our formulation is just the Murman-Cole problem.

References

[1] Landahl, M. T., *Unsteady Transonic Flow*, International Series of Monographs in Aeronautics and Astronautics, Pergamon Press, London, 1961.

[2] Cole, J. D., "Modern Developments in Transonic Flow," *SIAM Journal of Applied Mathematics*, Vol. 29, Dec. 1975, pp. 763-787.

Nonlinear Vibration of Beams with Variable Axial Restraint

Gangan Prathap*
Indian Institute of Technology, Madras, India

Nomenclature

$A(\xi), A_0$	= area at any station, reference station
$a(\xi)$	= nondimensional area variation
$I(\xi), I_0$	= moment of inertia at any station, reference station
$i(\xi)$	= nondimensional inertia variation
E	= modulus of elasticity
$F(t)$	= time function
$F_p(t), F_q(t)$	= summed up inertial forces at a station
H_B	= spring force
K	= nondimensional spring constant ($=kL/EA_0$)
k	= spring constant
L	= length of beam
M	= bending moment at any station
m_0	= mass per unit length of beam at reference station
N	= axial force at any station
$p(\xi)$	= distributed inertial force
Q	= shear force at any station
$q(\xi)$	= distributed inertial force
V_B	= vertical force at movable hinge
U, V	= displacements of a point on neutral axis in x,y directions
u, v	= U/L, V/L
x, y	= coordinate system
α	= $V_B L^2/EI_0$
γ	= $H_B L^2/EI_0$
ξ	= x/L, nondimensional coordinate
θ, θ_0	= slope at any station, at reference station
λ	= nondimensional quantity ($=m_0\omega^2 L^4/EI_0$)
ρ	= radius gyration at reference station
ω	= quantity characterizing vibration

I. Introduction

THE large-amplitude free flexural vibration of beams whose ends are restrained from axial displacement has received considerable attention.[1-5] The geometric nonlinearity is due to the axial force generated by stretching because of the immovability of the supports. The theory in Refs. 1-5 uses linearized curvature expressions and neglects the effect of longitudinal inertia and large deformation. The nonlinear behavior that results always is found to be of a hardening type; i.e., frequency increases with amplitude. A hinged beam, one end of which is immovable and the other movable, i.e., free of axial restraint, also was studied,[6-8] incorporating nonlinearities arising from longitudinal inertia, use of exact curvature expressions, and exact equilibrium equations (i.e., specification of loads in terms of the deformed configuration). The behavior in this case is of the softening type. Wrenn and Mayers[9] studied a general case of variable axial restraint, introducing the nonlinearity due to axial force alone. Thus, for the limiting case of infinite axial restraint, their results agree with those of beams on immovable supports,[1-5] whereas, for zero axial restraint, they obtain zero nonlinearity, contrary to the results reported in Refs. 6-8. Clearly, such a formulation must include the effects of longitudinal inertia and large curvatures. This Note therefore considers this general case, using a formulation in two displacement quantities developed in Ref. 10 and reported in Refs. 11 and 12.

Received Dec. 5, 1977; revision received Feb. 16, 1978.

Index category: Structural Dynamics.

*Research Assistant, Fibre Reinforced Plastics Research Centre.

II. Theory

From Fig. 1, the force equilibrium at station ξ is expressed as

$$N+F_p(\xi)\cos\theta+F_q(\xi)\sin\theta+H_B\cos\theta=V_B\sin\theta \tag{1}$$

$$Q+F_q(\xi)\cos\theta-F_p(\xi)\sin\theta-H_B\sin\theta=V_B\cos\theta \tag{2}$$

$$M,x-(1+\bar{\epsilon})Q=0 \tag{3}$$

where $F_p(\xi)$, $F_q(\xi)$ are the inertial forces summed up as

$$F_p(\xi)=L\int_\xi^1 p(\xi)\,d\xi, \quad F_q(\xi)=L\int_\xi^1 q(\xi)\,d\xi$$

and $\bar{\epsilon}$ is defined below. The differential equation of motion is obtained from Eqs. (2) and (3) as[10]

$$\frac{d}{d\xi}\left[i(\xi)\frac{d\theta}{d\xi}\right]+(1+\bar{\epsilon})\frac{L^2}{EI_0}\left[F_p(\xi)\sin\theta-F_q(\xi)\cos\theta+V_B\cos\theta+H_B\sin\theta\right]=0 \tag{4}$$

and the strain quantities $\epsilon=N/EA_0$, $\epsilon_0=V_B/EA_0$, and $\bar{\epsilon}=N/EA(\xi)$ are related as

$$\bar{\epsilon}=\frac{\epsilon}{a(\xi)}=\frac{\epsilon_0\sin\theta}{a(\xi)}-\frac{F_p(\xi)}{EA(\xi)}\cos\theta-\frac{F_q(\xi)}{EA(\xi)}\sin\theta-\frac{H_B}{EA(\xi)}\cos\theta \tag{5}$$

The analysis is simplified by assuming that $\bar{\epsilon}\ll 1$ within the elastic limit. Therefore, without much loss of accuracy, we have

$$U(\xi,t)=L\int_0^\xi(\cos\theta-1)\,d\xi \tag{6}$$

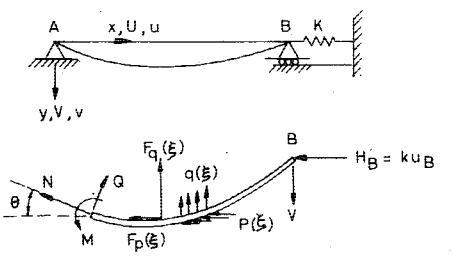

Fig. 1 Initial configuration and free body diagram at position of maximum amplitude.

$$V(\xi,t)=L\int_0^{\xi}\sin\theta d\xi \tag{7}$$

and, for a variable separable assumption, we have

$$\theta=\theta(\xi,t)=\bar{\theta}(\xi)F(t) \tag{8}$$

The key to the analysis that follows is the determination of the behavior of the system at the point of maximum amplitude. As the point of maximum amplitude (at time $t=t_1$, say) is a point of reversal of motion, the following properties of the time function are defined:

$$F(t_1)=1,\quad \frac{dF}{dt}(t_1)=0,\quad \frac{d^2F}{dt^2}(t_1)=-\omega^2 \tag{9}$$

We compute numerically a nondimensional quantity based on this value, ω^2, without any a priori assumption of the mode shape. The nonlinear behavior of the system then is interpreted in terms of the variation of this quantity with amplitude.

With these assumptions and definitions, one can obtain the equation of motion as the nonlinear integrodifferential equation:

$$\frac{d}{d\xi}\left[i(\xi)\frac{d\bar{\theta}}{d\xi}\right]+\lambda\left[\frac{\alpha}{\lambda}\cos\bar{\theta}+\cos\bar{\theta}Q(\xi)+\sin\bar{\theta}P(\xi)+\frac{\gamma}{\lambda}\sin\bar{\theta}\right]=0 \tag{10}$$

where $\alpha=V_BL^2/EI_0$, $\gamma=H_BL^2/EI_0$, $\lambda=m_0\omega^2L^4/EI_0$, and

$$P(\xi)=\int_{\xi}^{1}\left[a(\xi)\int_0^{\xi}\bar{\theta}\sin\bar{\theta}\,d\xi\right]d\xi \tag{11a}$$

$$Q(\xi)=\int_{\xi}^{1}\left[a(\xi)\int_0^{\xi}\bar{\theta}\cos\bar{\theta}\,d\xi\right]d\xi \tag{11b}$$

III. Solution

Equation (10) involves two undertermined constants, α and γ. These are determined by enforcing the boundary conditions in the following manner. From Eq. (7), one obtains

$$u_B=H_B/kL=\gamma/(L/\rho)^2K$$
$$=C(1)+\epsilon_0D(1)-[\gamma/(L/\rho)^2]E(1) \tag{12}$$

where

$$C(1)=\int_0^1\left\{\left(1-\frac{\lambda}{(L/\rho)^2}\frac{[P(\xi)\cos\bar{\theta}-Q(\xi)\sin\bar{\theta}]}{a(\xi)}\right)\cos\bar{\theta}-1\right\}d\xi$$

$$D(1)=\int_0^1\frac{\sin\bar{\theta}\cos\bar{\theta}}{a(\xi)}d\xi$$

$$E(1)=\int_0^1\frac{\cos^2\bar{\theta}}{a(\xi)}d\xi,\quad \alpha=\epsilon_0\left(\frac{L}{\rho}\right)^2$$

Therefore,

$$\frac{\gamma}{(L/\rho)^2}=\frac{K}{1+KE(1)}[C(1)+\epsilon_0D(1)] \tag{13}$$

The constant ϵ_0, or α, is determined next. Equation (10) is now recast as

$$\frac{d}{d\xi}\left[i(\xi)\frac{d\bar{\theta}}{d\xi}\right]=-\lambda\left[\int_0^{\xi}g(\xi)d\xi\right] \tag{14}$$

where

$$g(\xi)=h(\xi)+(\alpha/\lambda)\cos\bar{\theta}$$

$$h(\xi)=Q(\xi)\cos\bar{\theta}+P(\xi)\sin\bar{\theta}+(\gamma/\lambda)\sin\bar{\theta}$$

Integrating Eq. (14) and making use of the boundary condition $(d\bar{\theta}/d\xi)(0)=0$, one obtains

$$\frac{d\bar{\theta}}{d\xi}=-\lambda f(\xi) \tag{15}$$

where

$$f(\xi)=\left[\int_0^{\xi}g(\xi)d\xi\right]\Big/i(\xi)$$

The second boundary condition, $d\bar{\theta}/d\xi(1)=0$, and Eqs. (14) and (15) yield

$$\int_0^1\left[h(\xi)+\frac{\alpha}{\lambda}\cos\bar{\theta}\right]d\xi=0 \tag{16a}$$

or

$$\frac{\alpha}{\lambda}=\left[-\int_0^1h(\xi)d\xi\right]\Big/\left[\int_0^1\cos\bar{\theta}d\xi\right] \tag{16b}$$

Equation (15) now may be integrated to give

$$\bar{\theta}(\xi)=\theta_0-\lambda\int_0^{\xi}f(\xi)d\xi \tag{17}$$

For a given $\theta_0=\bar{\theta}(0)$, λ is obtained by solving the transcendental equation

$$V(1)-V(0)=\int_0^1\sin\left[\theta_0-\lambda\int_0^{\xi}f(\xi)d\xi\right]d\xi=0 \tag{18}$$

using a Newton-Raphson iteration scheme.

A numerically exact successive integration and iteration technique is used. A mode shape for $\bar{\theta}(\xi)$ is assumed first with $\bar{\theta}(0)=\theta_0$. Equations (13) and (16) are used to compute the quantities (γ/λ), (α/λ), and these values are used to solve for λ corresponding to the chosen θ_0 in Eq. (18). The improved mode shape for $\bar{\theta}(\xi)$ obtained from Eq. (17) is then used again; the iteration is repeated until λ,γ,α, and $\bar{\theta}(\xi)$, corresponding to the starting value of θ_0, converge to the required degree of accuracy.

IV. Results and Discussion

Numerical results are presented for a uniform beam. The computational procedure is quite accurate, and, for a division of the beam into 20 parts for purposes of numerical integration, the value of λ_0 obtained for linear theory (i.e., vanishing deflection $\theta_0\to0$) is 97.395; this compares well with the exact result, $\lambda_0=\pi^4=97.409$, i.e., an accuracy of 0.014%.

Figure 2 plots λ vs the nondimensional amplitude $\bar{V}/\rho$, where $\bar{V}=V(0.5)$, for two different values of slenderness ratio. For $K=0$, i.e., for zero axial restraint, only a softening type of behavior exists, as predicted.[6-8] Furthermore, the softening effect increases with decrease in slenderness ratio L/ρ. At $K=\infty$, a hardening type of behavior takes place, and this is independent of slenderness ratio.[1-5] However, these conclusions must be interpreted with care. If λ were plotted against $\bar{V}/L$ for $K=0$, the softening effect would be practically independent of L/ρ, as pointed out in Refs. 6-8, whereas the hardening effect then would depend on L/ρ. Therefore, for a beam of given slenderness ratio, there is some value of spring constant K at which there is a transition from the hardening to the softening type of behavior. The tran-

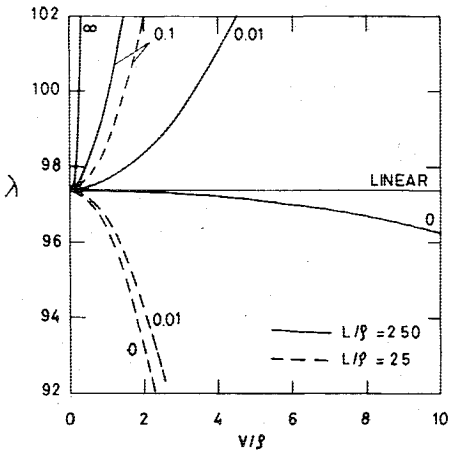

Fig. 2 λ-amplitude relationship.

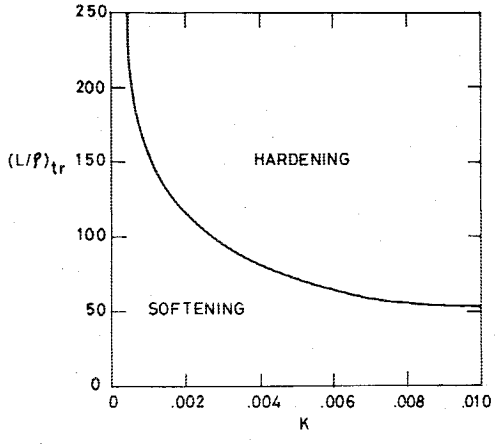

Fig. 3 Transition slenderness ratios vs spring constant.

sition value of (L/ρ) is plotted in Fig. 3 as a function of K. Thus we identify clearly a regime of a hardening type of nonlinear behavior and another of a softening type, depending on (L/ρ) and (kL/EA_0), for a uniform beam.

V. Conclusions

Whereas all previous analyses have studied the problem in the hardening regime alone[1-5,9] or in the softening regime alone,[6-8] this Note unifies both formulations. The variable axial restraint at the boundary is seen to play an important role in determining the nonlinear dynamic behavior of the beam. From the present results and earlier conclusions,[1-9] one may conclude that the principal causes and effects of nonlinearity are a hardening effect due to axial stretching, use of exact curvature expressions, and equilibrium equations, and a softening effect due to longitudinal inertia forces. At low values of spring constant and slenderness ratios, the effect of longitudinal inertia predominates, whereas, at high values of axial restraint and slenderness ratios, the effect of axial stretching predominates.

Acknowledgment

The author is deeply indebted to K. A. V. Pandalai and T. K. Varadan for their constant encouragement and interest in the subject.

References

[1] Woinowsky-Krieger, S., "The Effect of an Axial Force on the Vibration of Hinged Bars," *Journal of Applied Mechanics*, Vol. 17, 1950, pp. 35-36.

[2] Eringen, A., "On the Nonlinear Vibrations of Thin Bars," *Quarterly of Applied Mathematics*, Vol. 9, 1952, pp. 361-369.

[3] Burgreen, D., "Free Vibration of a Pin-Ended Column with Constant Distance Between Ends," *Journal of Applied Mechanics*, Vol. 18, 1951, pp. 135-139.

[4] Srinivasan, A. V., "Large Amplitude Free Oscillations of Beams and Plates," *AIAA Journal*, Vol. 3, Oct. 1965, pp. 1951-1953.

[5] Raju, I. S., Venkateshwara Rao, G., and Kanaka Raju, K., "Large Amplitude Free Vibrations of Tapered Beams," *AIAA Journal*, Vol. 14, Feb. 1976, pp. 280-282.

[6] Bolotin, V. V., *Dynamic Stability of Elastic Systems*, Holden-Day, 1964.

[7] Genin, J. and Radwan, H., "Nonlinear Bending Inertia of a Vibrating Beam," *Zeitschrift für Angewandte Mathematik und Physik*, Vol. 21, 1970, pp. 983-990.

[8] Atluri, S., "Nonlinear Vibrations of a Hinged Beam Inlcuding Nonlinear Inertia Effects," *Journal of Applied Mechanics*, Vol. 40, 1973, pp. 121-126.

[9] Wrenn, B. G. and Mayers, J., "Nonlinear Beam Vibrations with Variable Axial Boundary Restraint," *AIAA Journal*, Vol. 8, Sept. 1970, pp. 1718-1720.

[10] Prathap, G., "Nonlinear Behavior of Flexible Bars, Anisotropic Skew Plates and Stiffened Plates," Ph.D. Dissertation, Indian Inst. of Technology, Madras, India, 1977.

[11] Prathap, G. and Varadan, T. K., "Nonlinear Vibrations of Tapered Cantilevers," *Journal of Sound and Vibration*, Vol. 55, Jan. 1977.

[12] Prathap, G. and Varadan, T. K., "Large Amplitude Free Vibration of Tapered Hinged Beams," *AIAA Journal*, Vol. 16, Jan. 1978, pp. 88-90.

Radiometer Force on the Proof-Mass of a Drag-Free Satellite

Robert E. Jenkins*
The Johns Hopkins University, Laurel, Md.

Introduction

In recent years there has been increasing activity and interest in the use of "drag-free" and "accelerometric" satellites. Both of these devices make use of a proof-mass floating within a cavity, which is shielded by the cavity from air drag and solar radiation pressure forces. The idea was first proposed by Lange,[1] who also proposed various applications for such satellites.

The drag-free satellite is equipped with thrusters on the main satellite body which are operated by closed-loop control to keep the satellite body centered on the proof-mass. The entire spacecraft then, in principle, flies a purely gravitational orbit. The first such spacecraft, TRIAD (1972-69A), was successfully orbited by Johns Hopkins University/Applied Physics Lab in 1972.[2,3] The drag compensation system on TRIAD was based on a spherical, gold proof-mass in a spherical cavity, using a capacitance measurement to sense its position. A different, single-axis system has been recently orbited which is based on a doughnut-shaped proof-mass sliding along a wire. The proof-mass is suspended off the wire by radial magnetic forces, and its position is sensed optically. This system was used on the TIP Navigation Satellite launched in 1977.

In the accelerometric satellite, there is no thrusting system on the main body. Instead, a closed-loop control system maintains the proof-mass at the center of the cavity by means of an electrostatic internal force between the proof-mass and cavity. Ideally, this force just balances the external surface

Received Dec. 12, 1977; revision received Feb. 24, 1978.

Index categories: Spacecraft Dynamics and Control; Spacecraft Navigation, Guidance, and Flight-Path Control.

*Principle Professional Staff, Applied Physics Laboratory.